

---

# Contrastive Learning Via Equivariant Representation

---

Sifan Song<sup>1\*</sup>, Jinfeng Wang<sup>2,3\*</sup>, Qiaochu Zhao<sup>2</sup>, Xiang Li<sup>1</sup>, Dufan Wu<sup>1</sup>, Angelos Stefanidis<sup>2</sup>,

Jionglong Su<sup>2,†</sup>, S. Kevin Zhou<sup>4,†</sup>, Quanzheng Li<sup>1,†</sup>

<sup>1</sup> Center for Advanced Medical Computing and Analysis (CAMCA),  
Massachusetts General Hospital and Harvard Medical School, Boston, USA  
<sup>2</sup> School of AI and Advanced Computing, XJTLU Entrepreneur College (Taicang),  
Xi'an Jiaotong-liverpool University, Suzhou, China  
<sup>3</sup> University of Liverpool, Liverpool, UK  
<sup>4</sup> School of BME & Suzhou Institute for Advanced Research,  
Center for Medical Imaging, Robotics, Analytic Computing & Learning (MIRACLE),  
University of Science and Technology of China, Suzhou, China

## Abstract

Invariant-based Contrastive Learning (ICL) methods have achieved impressive performance across various domains. However, the absence of latent space representation for distortion (augmentation)-related information in the latent space makes ICL sub-optimal regarding training efficiency and robustness in downstream tasks. Recent studies suggest that introducing equivariance into Contrastive Learning (CL) can improve overall performance. In this paper, we rethink the roles of augmentation strategies and equivariance in improving CL efficacy. We propose a novel Equivariant-based Contrastive Learning (ECL) framework, CLeVER (Contrastive Learning Via Equivariant Representation), compatible with augmentation strategies of arbitrary complexity for various mainstream CL methods and model frameworks. Experimental results demonstrate that CLeVER effectively extracts and incorporates equivariant information from data, thereby improving the training efficiency and robustness of baseline models in downstream tasks. *Code is available at <https://github.com/SifanSong/CLeVER>*

## 1 Introduction

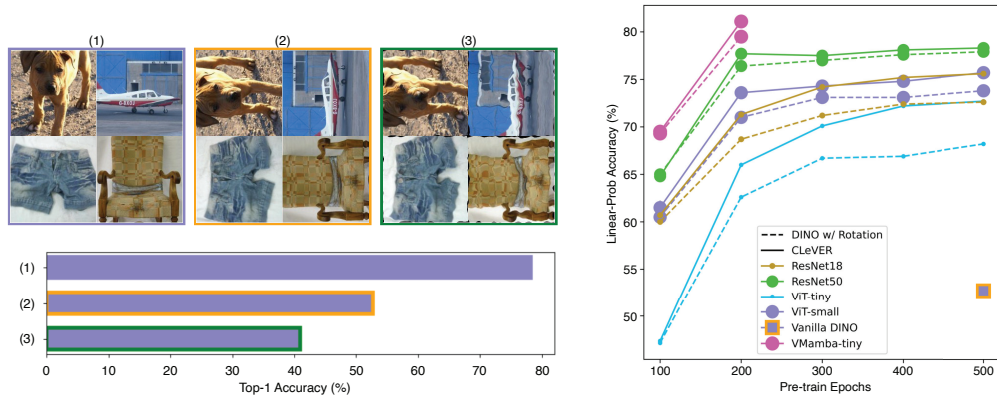
Self-supervised learning (SSL) reveals the relationships between different views or components of the data to produce labels inherent to the data. These labels serve as supervisors for pretext tasks in the pre-training process [16]. As an unsupervised training strategy, SSL eliminates the reliance on manual labeling, enabling SSL-based methods to achieve superior performance and promising generalization capabilities across many domains [4, 11, 16, 21].

As a critical methodology in the SSL community, Invariant Contrastive Learning (ICL) generates different views of the same input instance through data augmentation, expecting the backbone model to extract semantic-invariant representations from the different distorted views. However, this semantic-invariance-based approach assumes that only semantics unrelated to the distortions brought by augmentation operations are valuable. In other words, typical ICL methods discard representations affected by augmentation operations. This assumption necessitates careful construction of

---

\*These authors contributed equally to this work.

†Corresponding authors: Jionglong Su (Jionglong.Su@xjtlu.edu.cn), S. Kevin Zhou (skevinzhou@ustc.edu.cn), Quanzheng Li (Li.Quanzheng@gh.harvard.edu)



(a) Comparison of DINO [4] performance in the face of different perturbations: (1) The samples are in common orientations and states. (2) The samples are in an uncommon orientation and rotated. (3) The samples are in unusual orientations and imaging states. (b) Comparison of the performance of various backbone models pre-trained with CLeVER and DINO on ImageNet-100. All performances are obtained under rotational perturbation.

Figure 1: CLeVER can introduce a comprehensive robustness improvement for DINO.

augmentation strategies to achieve optimal downstream performance [5]. Moreover, such exquisite augmentation strategies make pre-trained models vulnerable to unseen perturbations, as shown in Fig. 1(a).

As the counterpart to the invariant principle, equivariant-based deep learning is well-studied [2, 13, 32, 24, 30]. Theoretically, a model can learn to be invariant or equivariant as required by the task for which it is trained [30]. That is, a model can acquire the invariant or equivariant properties necessary for a task by sufficiently training on a task-specific dataset. However, a naive model needs to explicitly learn these properties, *i.e.*, it needs to be presented with as many possible transformed states (e.g., poses or positions) to understand the equivariant relationships among these states. This naive approach leads to low training efficiency, high data requirements, weak generalization ability, and non-robustness, which are undesirable. Consequently, many works have emerged that aim to design structurally constrained models by incorporating equivariance [30]. Instead of repeatedly learning different views of the same sample, these models automatically generalize their knowledge to all considered transformations. These equivariant-based models typically reduce the number of parameters, complexity, and data requirements while improving training efficiency, prediction performance, generalization, and robustness.

However, the aforementioned work on equivariant-based model design focuses on supervised learning and task-specific scenarios. As an unsupervised learning and general-purpose pre-training strategy, the CL approach cannot realize the introduction of the equivariant properties by changing the structural design of the backbone model or the prediction head. Moreover, since the training process of CL deals with pretext tasks, the desired task-specific equivariance in the downstream task remains unknown. Some recent work based on Equivariant-based Contrastive Learning (ECL) introduces rotational equivariance by integrating rotation into the augmentation strategy and incorporating temporary modules or architectures into the CL pre-training process [1, 31, 9, 10, 27]. However, such works all assume that rotational equivariance is a generic property of downstream tasks, making it challenging to introduce more complex equivariance. Notably, a recent study, named distortion-disentangled contrastive learning (DDCL) [27], proposes an adaptive design that splits output representations and explicitly projects the distortions caused by augmentation into a latent space, thereby leveraging information from the augmentation. Since this method does not require distortion-specific modules and architectures, it can be easily extended to more complex augmentation strategies to introduce more complicated equivariance. However, due to the vulnerability of the orthogonal loss introduced by DDCL, its training process is unstable and easily leads to trivial solutions. Therefore, the following sections rethink both the ECL framework and the DDCL method in detail and propose our novel ECL framework, named CLeVER.

In summary, our main contributions are as follows:

- We rethink the ECL framework and DDCL, and propose a regularization loss for projection heads to prevent them from collapsing and generating trivial solutions when extracting equivariant representations using orthogonal loss.
- We propose a novel ECL framework, CLeVER, based on our proposed projection head regularization loss and the advanced ICL framework DINO [4]. CLeVER improves the performance of backbones by adaptively introducing equivariance using augmentation strategies of arbitrary complexity.
- Our proposed CLeVER significantly improves the training efficiency, generalization, and robustness of CL. Additionally, we find that CLeVER is able to boost the performance of small and medium-scale backbones.
- We employ CLeVER for three mainstream backbone models (ResNet [17], ViT [12], and VMamba [19]), as illustrated in Fig. 1(b), experimentally demonstrating that various types of backbone models can achieve better performance with CLeVER. Interestingly, we find that VMamba-based contrastive learning has outstanding performance on medium-scale data.

## 2 Rethink the Equivariant Representation in CL

Although ICL methods are widely used, the assumption or inductive bias of focusing only on semantic information unrelated to augmentations/distortions raises some potential concerns. To achieve semantic invariant representation in ICL methods, the backbone model needs to learn as many views of the same sample as possible to achieve the multi-view-to-unique-feature mapping, potentially reducing training efficiency. In other words, the backbone model needs to memorize as many views as possible for each sample, leading to small-scale models failing to achieve satisfactory performance in ICL. In addition, since typical ICL methods disregard all information associated with augmentations/distortions, the backbone model may exhibit poor generalization in downstream tasks that require such semantic information (*e.g.*, color semantics are crucial for classifying food and plants). Furthermore, since ICL methods often carefully select augmentation operations to achieve the best performance scores in common scenarios, pre-trained backbone models lack robustness against certain unknown perturbations. For example, due to the difficulty of achieving rotational invariance, ICL methods typically avoid choosing rotation as an augmentation operation. As shown in Fig. 1(a), this trade-off results in ICL methods generally struggling to handle rotation as a common perturbation effectively.

Recent studies [1, 31, 9, 10, 27] have introduced equivariance into CL methods and proposed several ECL frameworks to address the aforementioned concerns. Although the principles of these works are diverse, these works share several concerns. First, these frameworks usually focus only on realizing contrastive learning with rotational equivariance, which means they focus on only a sub-problem of ECL, thereby limiting their extensibility and potential. Second, these studies employ some equivariant-specific architectures or pretext task designs, such as adding rotation predictor heads during pre-training to achieve rotation sensitivity [9]. Such equivariant-specific designs rely on manual labor and drag down training efficiency. Third, these works have not validated the performance of different types and scales of backbone models within their frameworks, which is concerning as a general-purpose pre-training framework.

DDCL [27] differs from the aforementioned ECL frameworks that rely on equivariant-specific architecture and pretext task designs. It adopts a representation disentanglement approach, explicitly splitting the output of a backbone model into distortion-invariant and distortion-variant representations, and introduces an orthogonal loss function to adaptively disentangle the distortion-variant representation. By explicitly leveraging both distortion-variant and distortion-invariant semantic information, DDCL significantly improves training efficiency and robustness. More importantly, since DDCL adaptively extracts distortion-variant representations, it can be easily adapted to augmentation strategies of arbitrary complexity. However, our in-depth study of DDCL reveals several drawbacks. We find that the orthogonal loss proposed by DDCL is vulnerable and may generate trivial solutions. Although it is reasonable to utilize an orthogonal loss to disentangle the distortion-variant representation from different augmented views, DDCL’s straightforward and unsupervised projection head for the distortion-variant representation tends to collapse to zero values during training on medium and large-scale datasets. This leads to an unstable training process for DDCL and makes

Table 1: Order of magnitude of the parameters and output representations of the projection head during pre-training in ImageNet-1K [23] by the DDCL (w/ and w/o proposed  $L_{PReg}$ ).  $h_{V/I}$  and  $z_{V/I}$  refer to the parameters of the head and representations respectively. All values are scaled by  $\log_{10}(\cdot)$ .

Methods	DDCL w/o $L_{PReg}$				DDCL w/ $L_{PReg}$			
	$h_V$	$h_I$	$z_V$	$z_I$	$h_V$	$h_I$	$z_V$	$z_I$
10	-1.46	2.04	-5.08	-0.32	1.87	1.87	-0.23	-0.45
50	-9.63	2.13	-9.84	-0.38	1.91	1.91	-0.26	-0.53
100	-17.1	2.09	-13.8	-0.53	1.85	1.85	-0.20	-0.71
200	-21.1	1.83	-18.6	-1.46	1.60	1.60	-1.37	-1.87
Status	Collapse / Trivial Solution				Similar projection			

it difficult to be further utilized. Moreover, has not yet explored its performance across different backbone models, leaving its generalizability currently unverified.

### 3 Proposed Methods

Inspired by DDCL, we follow its methodology and employ an orthogonal loss function to supervise equivariant representations in the latent space for the ICL framework. In addition, based on the framework of DDCL, we propose a new regularization loss for the projection head to address the instability of DDCL. Furthermore, we incorporate DINO [4] as a baseline because it is not only a widely recognized method but also more stable and can support more mainstream backbone models. By integrating equivariant representations into DINO through our stabilized DDCL, we propose a novel equivariant-based contrastive learning method, CLeVER (Contrastive Learning Via Equivariant Representation). Moreover, we validate the training efficiency and robustness of CLeVER across various mainstream backbone models.

#### 3.1 Make DDCL Stable

DDCL [27] explicitly splits the output representation of the backbone model into distortion-invariant and distortion-variant representations. The contrastive and orthogonal losses are used to supervise the pairwise distortion-invariant and pairwise distortion-variant representations across different views during the contrastive process, respectively. The formula for this process is formulated as follows:

$$z_I^{(1,2)}, z_V^{(1,2)} = f(t_{1,2} \circ I) \quad (1)$$

$$L_I = L_{CL}(h_I(z_I^{(1)}), h_I(z_I^{(2)})) = -\text{Similarity}(h_I(z_I^{(1)}), h_I(z_I^{(2)})) \quad (2)$$

$$L_V = L_{Orth}(h_V(z_V^{(1)}), h_V(z_V^{(2)})) = h_V(z_V^{(1)}) \cdot h_V(z_V^{(2)}) \quad (3)$$

$$L_{DDCL} = \alpha L_I + \beta L_V \quad (4)$$

where  $f(\cdot)$  is the backbone model of contrastive learning. The subscripts  $I$  and  $V$  refer to the variables or functions used for distortion-invariant and distortion-variant representations, respectively, and superscripts 1 and 2 represent two views of the same sample.  $z$  and  $h$  refer to the representation in the latent space and the projection head in the pretext task, respectively.

Analyzing the loss function of the distortion-variant representation of DDCL (*i.e.*, Eq. 3), we find that DDCL attempts to de-correlate the projected vectors of pairwise distortion-variant representations by making them orthogonal to each other. However, the orthogonality of  $h_V(z_V^{(1)})$  and  $h_V(z_V^{(2)})$  is not sufficiently necessary for  $L_{Orth}$  to reach zero. We find that when training DDCL on a medium and large-scale dataset, the parameter values of the projection head ( $h_V(\cdot)$ ) tend to zero, generating zero values for the projected vectors ( $h_V(z_V^{(1)})$  and  $h_V(z_V^{(2)})$ ). This trivial solution should be considered as a collapsed projection to a null space rather than achieving orthogonality between representations. Consequently, the split distortion-variant representations may not be effectively supervised and disentangled as expected.

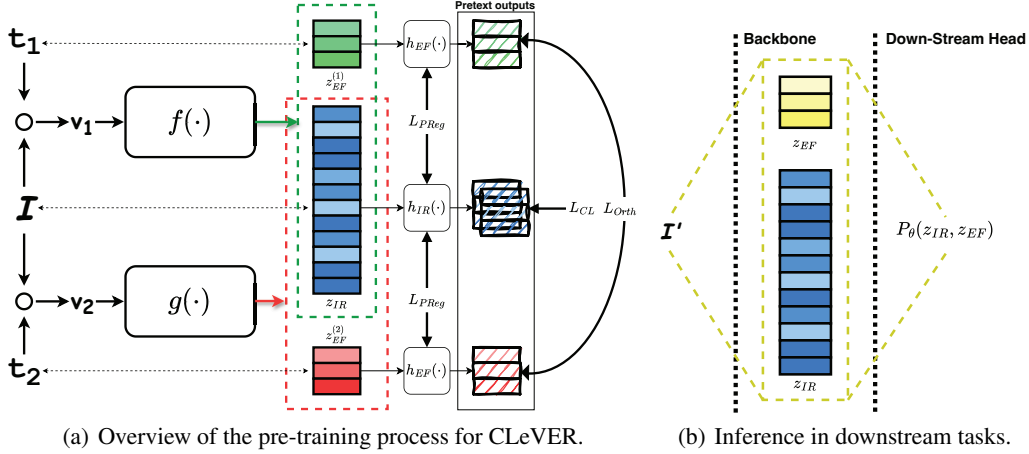


Figure 2: A brief overview of the working process of CLeVER. (a)  $f(\cdot)$  and  $g(\cdot)$  are backbone models. In DINO, they are EMA-based (Exponential Moving Average) teacher-student relationships. All  $z_{EF}$  represent equivariant factors in the latent space corresponding to transformation operations  $t_1$  and  $t_2$ , and  $z_{IR}$  is denotes invariant representation of the invariant semantics in the latent space.  $h$  represents the projection head used in the pretext task. In CLeVER, the loss of contrastive learning ( $L_{CL}$ ) of the baseline method, the loss of orthogonality ( $L_{Orth}$ ), and the projection regularization loss ( $L_{PReg}$ ) are used. (b) In downstream tasks, the disentangled invariant representation and equivariant factor from the pre-trained backbone are incorporated for inference and prediction.

To address the trivial solution of  $L_{Orth}$ , we propose a novel regularization loss,  $L_{PReg}$ , for the projection head. This loss function ensures that the parameter magnitude of  $h_V$  is aligned with that of  $h_I$ , thereby preventing the collapse of  $h_V$ . The proposed loss function is formulated as follows:

$$L_{PReg} = L_1(\|h_V\|_2^2, \|h_I\|_2^2) = \left| \|h_V\|_2^2 - \|h_I\|_2^2 \right| \quad (5)$$

where  $L_1(\cdot)$  is the L1 loss function,  $\|\cdot\|_2^2$  refers to the L2 norm. As demonstrated in Table 1,  $L_{PReg}$  effectively stabilize DDCL by preventing training collapse and avoiding trivial solutions.

### 3.2 CLeVER

To introduce equivariant representations into contrastive learning and thereby improve the training efficiency, robustness, and generalizability of the backbone model, we rethink the definition of equivariance. Given a transformation group  $T$  with group actions  $t \triangleright_X$  and  $t \triangleright_Y$  in domain  $X$  and co-domain  $Y$ , respectively, we consider a function  $f : X \rightarrow Y$  to be  $T$ -invariant when it satisfies Eq. 6. We call it  $T$ -invariance when  $f$  satisfies Eq. 7. Obviously,  $T$ -invariance is a trivial case of  $T$ -equivariance (when  $t \triangleright_Y := id_Y$ ).

$$f(t \triangleright_X x) = f(x) \quad \forall t \in T, x \in X \quad (6)$$

$$f(t \triangleright_X x) = t \triangleright_Y f(x) \quad \forall t \in T, x \in X \quad (7)$$

Assuming that the group  $T$  has another group operation  $t \triangleright'_Y = id_Y$  (identify operation) in the co-domain, Eq. 7 can be modified as follows:

$$f(t \triangleright_X x) = t \triangleright_Y f(x) = t \triangleright_Y (t \triangleright'_Y f(x)) \quad \forall t \in T, x \in X \quad (8)$$

Up to here, we can consider that when the transformation operation  $t \in T$  perturbs the input  $x \in X$  according to the group action  $t \triangleright_X$ , we can introduce  $T$ -equivariance by finding a proper group action  $t \triangleright_Y$  to attribute the effect caused by  $t$  to the representation  $f(x)$  which is  $T$ -invariant in the co-domain  $Y$  (latent space).

As illustrated in Fig. 2(a), we refer to the framework design of DDCL to explicitly split the representations extracted from the backbone model into **Invariant Representations** ( $z_{IR}$ ) and **Equivariant Factors** ( $z_{EF}$ ) according to a predefined separation ratio. Furthermore,  $z_{IR}$  and  $z_{EF}$  are supervised, respectively, using the contrastive loss ( $L_{CL}$ ) and orthogonal loss ( $L_{Orth}$ ), with the help of the projection regularization loss ( $L_{PReg}$ ). The group action  $t \triangleright_Y$  of the group  $T$  in the co-domain  $Y$  is realized as a concatenation operation, and a trainable neural network that is parallel to and shares some parameters with the backbone model  $f$ . We name the framework CLeVER, an abbreviation for Contrastive Learning Via Equivariant Representation. The formulas are given as follows:

$$(z_{IR}^{(1,2)}, z_{EF}^{(1,2)}) = t \triangleright_Y f(x) = f(t_{1,2} \triangleright_X x) \quad \forall t \in T, x \in X \quad (9)$$

$$L_{CL} = CE(\text{Softmax}(h_{IR}(z_{IR}^{(1)})), \text{Softmax}(h_{IR}(z_{IR}^{(2)}))) \quad (10)$$

$$L_{Orth} = \text{Softmax}(h_{EF}(z_{EF}^{(1)})) \cdot \text{Softmax}(h_{EF}(z_{EF}^{(2)})) \quad (11)$$

$$L_{PReg} = |||h_{EF}||_2^2 - ||h_{IR}||_2^2| \quad (12)$$

$$L_{Total} = \alpha L_{CL} + \beta L_{Orth} + \lambda L_{PReg} \quad (13)$$

In the training process of CLeVER, we retain the principle of extracting representations invariant to augmentation operations as used in ICL approaches. Furthermore, we incrementally extract representations that can be used to represent the effects of distortion or perturbation for the samples in a learnable manner. This means that CLeVER only provides information about the perturbations without introducing inductive biases or assumptions a priori (*e.g.*, sensitivity or robustness to a specific perturbation). Unlike other CL methods, CLeVER explicitly splits the extracted representations into invariant representations ( $z_{IR}$ ) and equivariant factors ( $z_{EF}$ ). Thus, during the inference process (*e.g.*, for a classification task), the prediction head of the downstream task performs a joint probabilistic prediction, *i.e.*,  $P_\theta(z_{IR}, z_{EF})$ , based on  $z_{IR}$  and  $z_{EF}$ , as illustrated in Fig. 2(b). This joint modeling allows the downstream tasks to leverage both invariant and equivariant information, enhancing the robustness and generalization of the model.

### 3.3 Make All Backbones CLeVER

In this paper, to comprehensively validate the generalizability of CLeVER, we select three kinds of representative mainstream backbone models: ResNet [17], ViT [12], and VMamba [19], based on convolutional operators, self-attention operators, and selective state space models, respectively. Additionally, we use different sizes of backbone models, pre-training datasets, and downstream datasets to investigate CLeVER’s training efficiency, performance, and robustness. We mainly incorporate DINO [4] as the basic framework since it supports more mainstream backbone models and is more stable than SimSiam [6].

In addition, although this paper does not focus on the effect of the variety of data augmentation strategies on CLeVER, it is noteworthy that CLeVER is fully adaptive and does not require any augmentation-specific design. This suggests that CLeVER can enrich the equivariance of backbone models by increasing the complexity of the augmentation strategy and incorporating more varieties of transformations.

## 4 Experiments

### 4.1 Implementation Details

We use ImageNet-1K (IN-1k) and ImageNet-100 (IN-100) for pre-training, with IN-100 serving as our default pre-training dataset over 500 epochs. In addition, we evaluate the performance of CLeVER on both in-domain and out-of-domain downstream tasks. For in-domain downstream tasks

(1% and 10% semi-supervised learning), we use the same dataset as in pre-training (IN-1k or IN-100). For out-of-domain downstream tasks, we use CUB200 [26], Flowers102 [20], Food101 [3], and OxfordPet [22] for downstream classification tasks. Additionally, for out-of-domain segmentation downstream tasks, we use DAVIS 2017 [25], ECSSD [28], DUTS [33], and DUT\_OMRON [29] as test sets. All experiments are conducted on four NVIDIA A100 (80G) GPUs, with experimental setups identical to those of DINO [4] and DDCL [27] (details in Appendix 5.2).

In this paper, we report on three data augmentation strategies: Basic Augmentation (BAug), Complex Augmentation (CAug), and High Complexity Augmentation (CAug+). We refer to the data augmentation strategies (including color jittering, Gaussian blur, solarization, and multi-crop) used by DINO, as BAug. Furthermore, we refer to DDCL using BAug with the addition of rotation as CAug, and CAug with the addition of elastic transformation as CAug+ (details in Appendix 5.3).

## 4.2 Robustness of Equivariance

To validate the positive impact of equivariance on the robustness of the backbone model, we use perturbed test data in the linear evaluation of the pre-trained backbone model with perturbations. In this experiment, in addition to CLeVER based on DINO, we also include Simsim [6], referring to DDCL, as a baseline to validate the effect of our proposed projection regularization. In this paper, Orig. denotes no perturbation (*i.e.*, linear evaluation), CJ represents color jitter, Ro and ET denote rotation and elastic transformations, respectively. ‘-IR’ denotes that only split Invariant Representations of the backbone (*i.e.*,  $z_{IR}$ ) are used for evaluation.

The  $L_{PReg}$ -related experiments in Table 2 demonstrate that our proposed projection regularization loss improves the robustness of DDCL. This improvement may be attributed to  $L_{PReg}$  preventing training collapse and increasing the disentanglement efficiency of DDCL. More importantly, the evaluation results in Table 2 and 3 suggest that Equivariant Factors (*i.e.*,  $z_{EF}$ ) can effectively improve the robustness of ICL approaches. With Simsim as the baseline, introducing stable equivariance improves the performance of the backbone under the perturbation of rotation and elastic transformation by about 27% and 48%, respectively. Similarly, by incorporating equivariance, CLeVER improves the performance of vanilla DINO under perturbations of rotation and elastic transformation by about 21% and 31%, respectively.

Table 2: The effect of equivariance on the robustness of Simsim

Methods	Orig.	CJ	CJ+Flip	CJ+Ro	CJ+Ro+ET
Trained by BAug					
Simsim [6]	81.9	81.3	81.4	50.3	27.3
DDCL [27]	82.2	81.6	<b>81.6</b>	50.0	26.8
DDCL-IR w/ $L_{PReg}$	82.2	81.5	81.4	51.9	27.7
DDCL w/ $L_{PReg}$ (Ours)	<b>82.3</b>	<b>81.8</b>	<b>81.6</b>	51.6	27.3
Trained by CAug (w/ Ro)					
Simsim	79.7	79.0	79.0	77.0	51.9
DDCL	80.0	79.3	79.4	77.2	48.5
DDCL-IR w/ $L_{PReg}$	80.3	79.6	79.5	<b>77.6</b>	48.2
DDCL w/ $L_{PReg}$ (Ours)	<b>80.7</b>	<b>80.2</b>	<b>80.0</b>	<b>77.6</b>	48.1
Trained by CAug+ (w/ Ro and ET)					
Simsim	78.6	77.7	77.7	75.1	74.1
DDCL	78.8	78.2	78.2	75.4	74.2
DDCL-IR w/ $L_{PReg}$	79.6	78.8	78.9	76.8	75.4
DDCL w/ $L_{PReg}$ (Ours)	<b>79.8</b>	<b>79.0</b>	<b>79.3</b>	<b>77.0</b>	<b>75.5</b>

Table 3: The effect of equivariance on the robustness of DINO

Methods	Orig.	CJ	CJ+Flip	CJ+Ro	CJ+Ro+ET
Trained by BAug					
DINO [4]	78.2	77.6	77.2	52.7	41.0
CLeVER-IR	<b>78.5</b>	77.2	77.5	52.4	41.7
CLeVER (Ours)	78.3	<b>77.8</b>	<b>78.1</b>	53.4	41.2
Trained by CAug (w/ Ro)					
DINO	76.0	74.7	75.2	73.8	63.4
CLeVER-IR	77.3	75.8	76.4	75.2	65.2
CLeVER (Ours)	<b>77.5</b>	<b>75.9</b>	<b>76.5</b>	<b>75.7</b>	64.8
Trained by CAug+ (w/ Ro and ET)					
DINO	73.9	73.4	73.2	72.3	69.4
CLeVER-IR	<b>75.5</b>	<b>74.2</b>	73.8	73.6	70.4
CLeVER (Ours)	75.2	74.0	<b>74.5</b>	<b>73.8</b>	<b>71.7</b>

## 4.3 Downstream Tasks

We use the pre-trained backbone model for in-domain and out-of-domain downstream tasks to evaluate the generalization ability of CLeVER. The results in Table 4 show that CLeVER improves the efficiency of in-domain semi-supervised learning compared to DINO. In addition, in the out-of-domain downstream classification tasks, CLeVER provides more significant improvement when pre-trained with complex augmentation strategies.

To validate the impact of introducing equivariance on attention and performance in downstream segmentation tasks, we conduct unsupervised video target segmentation tests referring to DINO. We also perform unsupervised saliency segmentation tests based on TokenCut [29]. The results in Table 5 indicate that CLeVER significantly improves unsupervised segmentation performance. Moreover, the use of complex augmentation strategies and equivariance notably improve the backbone model’s segmentation capabilities.

Table 4: In-domain and out-of-domain downstream classification tasks

Methods	In-domain Semi.		Out-of-domain Downstream			
	1%	10%	CUB200	Flowers102	Food101	OxfordPet
Trained by BAUG						
DINO	57.9	<b>75.1</b>	62.4	<b>80.6</b>	82.2	79.0
CLeVER	<b>59.5</b>	75.0	61.6	79.4	82.4	<b>79.7</b>
Trained by CAUG (w/ Ro)						
DINO	53.5	72.7	62.4	80.2	82.9	76.2
CLeVER	<b>56.3</b>	<b>74.9</b>	<b>63.2</b>	80.4	<b>83.0</b>	78.1

Table 5: Unsupervised downstream segmentation tasks

Methods	Video object seg.			Unsupervised saliency seg.					
	DAVIS 2017			ECSSD		DUTS		DUT_OMRON	
	$(J&F)_m$	$J_m$	$F_m$	IoU	Acc.	IoU	Acc.	IoU	Acc.
Trained by BAUG									
DINO	0.594	0.582	0.606	0.657	0.866	0.431	0.789	0.427	0.780
CLeVER	0.592	0.577	0.606	0.673	0.877	0.440	0.801	0.443	0.787
Trained by CAUG (w/ Ro)									
DINO	0.602	0.582	0.623	0.655	0.867	0.426	0.784	0.417	0.766
CLeVER	<b>0.607</b>	<b>0.586</b>	<b>0.628</b>	<b>0.688</b>	<b>0.888</b>	<b>0.446</b>	<b>0.803</b>	<b>0.447</b>	<b>0.789</b>

To explore the role of equivariant factors during inference, we use the CAUG-based pre-trained backbone model for rotational invariance and rotational sensitivity testing. In rotational invariance testing, we randomly rotate the OxfordPet data between  $\pm 90^\circ$  and  $\pm 180^\circ$ . The rotated data are then used for evaluation in a downstream classification task. In rotational sensitivity testing, we perform a 4-fold rotation prediction ( $90^\circ$ ,  $180^\circ$ ,  $270^\circ$ , and  $360^\circ$ ) on OxfordPet data. The accuracy of the predicted rotation degrees is then evaluated as a downstream task to assess the backbone’s rotational sensitivity.

The experiments in Tables 6 and 7 demonstrate that the equivariant factors extracted by CLeVER do not introduce inductive bias as the vanilla architecture but instead provide perturbation-related information. This information can be utilized in various ways depending on the requirements of downstream tasks, resulting in improved rotational invariance or rotational sensitivity.

Table 6: Experiments of rotational invariance

Methods	Linear			Fine-tune		
	Orig.	Ro.(90°)	Ro.(180°)	Orig.	Ro.(90°)	Ro.(180°)
DINO	65.3	62.6	61.3	76.9	68.5	65.6
CLeVER	<b>67.1</b>	<b>63.4</b>	<b>62.3</b>	<b>78.7</b>	<b>69.9</b>	<b>66.9</b>

Table 7: Rotational sensitivity

Methods	Linear	Fine-tune
DINO	52.2	75.2
CLeVER	<b>53.2</b>	<b>75.5</b>

#### 4.4 Generalizability of CLeVER

We employ several mainstream backbone models to study the generalizability of CLeVER and the impact of equivariance on different backbone models. We also compare CLeVER with some popular ICL approaches. Each linear experiment of DINO and CLeVER is repeated five times. The results in Table 8 indicate that CLeVER improves the performance of DINO across various types and scales of backbone models. Notably, smaller-scale models gain more significantly from the introduction of equivariance. Interestingly, VMamba [19], a recently proposed backbone model, can be effectively integrated into the framework to achieve outstanding performance. Fig. 1(b) and Table 8 further demonstrate that VMamba has surprising performance gains from equivariance within the CLeVER framework. This suggests that the integration of equivariant factors not only improves robustness and generalization but also maximizes the potential of innovative backbone architectures like VMamba.

#### 4.5 CLeVER in Large-scale Dataset

We conduct a robustness experiment of CLeVER on the large dataset IN-1k to validate its reliability. In this experiment, we use ViT-Small as the backbone model and pre-train it for 100 epochs. Table 9 indicates that on the large dataset, CLeVER can still improve the robustness of the backbone model by increasing the complexity of the augmentation strategy, although the performance gain is not as pronounced as on the medium-scale dataset, IN-100. We believe this may be due to the fact that in large datasets, a substantial amount of semantic information exists for the backbone model to learn, making the learning of equivariance more challenging. Furthermore, the “Trained by CAUG+” part in Table 9 suggests that the gains from equivariance become progressively more significant as the

Table 8: Comparison of linear performance of models pre-trained on IN-100 over 200 epochs. CLeVER and approaches with (R) represent that they are pre-trained with rotated images. The green numbers represent performance increases compared to the corresponding DINO-based backbones.

Methods	Handle R.	Backbones	#Params	GFLOPs	Top-1	<i>std.</i>	Top-5
SimCLR [5]	✗	ResNet50	23.5M	4.14G	73.6	-	-
SimCLR (R)	✓	ResNet50	23.5M	4.14G	72.9	-	-
Debiased [8]	✗	ResNet50	23.5M	4.14G	74.6	-	92.1
BYOL [15]	✗	ResNet50	23.5M	4.14G	76.2	-	93.7
MoCo [18]	✗	ResNet50	23.5M	4.14G	73.4	-	-
MoCo v2 [7]	✗	ResNet50	23.5M	4.14G	78.0	-	-
MoCo v2 (R)	✓	ResNet50	23.5M	4.14G	72.0	-	-
RefosNet (MoCo v2) [1]	✓	ResNet50	23.5M	4.14G	80.5	-	95.6
	✓	ViT-Tiny	5.5M	1.26G	66.2	±0.086	89.0
	✓	ResNet18	11.2M	1.83G	71.5	±0.066	91.8
DINO (R)	✓	ViT-Small	21.7M	4.61G	73.2	±0.161	92.7
	✓	ResNet50	23.5M	4.14G	78.4	±0.130	94.9
	✓	VMamba-Tiny	29.5M	4.84G	80.9	±0.092	95.7
	✓	ViT-Tiny	5.5M	1.26G	68.7 <sub>+2.5</sub>	±0.087	90.7
	✓	ResNet18	11.2M	1.83G	74.2 <sub>+2.7</sub>	±0.068	92.9
CLeVER	✓	ViT-Small	21.7M	4.61G	75.7 <sub>+2.5</sub>	±0.107	93.6
	✓	ResNet50	23.5M	4.14G	79.1 <sub>+0.7</sub>	±0.097	95.4
	✓	VMamba-Tiny	29.5M	4.84G	83.0 <sub>+2.1</sub>	±0.072	96.4

complexity of the perturbations increases. This highlights the importance of incorporating complex augmentation strategies to maximize the robustness improvements offered by equivariance, even in large and information-rich datasets.

Table 9: Robustness performance in ImageNet-1k

Methods	Orig.	CJ	CJ+Flip	CJ+Ro	CJ+Ro+ET
	Trained by BAUG				
DINO	<b>73.5</b>	72.6	<b>72.8</b>	48.2	32.6
CLeVER	<b>73.5</b>	<b>72.7</b>	72.6	48.0	31.8
	Trained by CAUG (w/ Ro)				
DINO	71.8	70.9	70.9	70.0	55.6
CLeVER	<b>72.0</b>	<b>71.2</b>	<b>71.2</b>	<b>70.1</b>	55.3
	Trained by CAUG+ (w/ Ro and ET)				
DINO	70.2	69.3	69.3	68.3	66.4
CLeVER	<b>70.7</b>	<b>69.9</b>	<b>69.8</b>	<b>69.0</b>	<b>66.8</b>

#### 4.6 Ablation Study

In this subsection, we perform ablation studies on some critical hyperparameters within CLeVER to ensure optimal configurations. Fig. 3(a) shows that the optimal separation ratio (*i.e.*, the ratio of the dimensions of  $z_{IR}$  and  $z_{EF}$ ) is 0.8. Fig. 3(b) demonstrates that the optimal choice of the output dimension for the projection head in CLeVER is the default  $2^{16} = 65536$ . Fig. 3(c) shows that the optimal weight  $\lambda$  for  $L_{PReg}$  is 0.001.

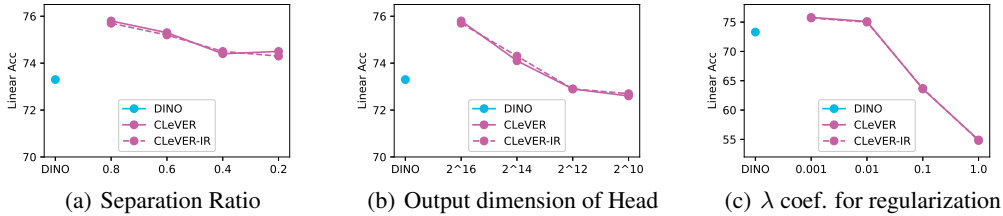


Figure 3: Ablation studies on hyperparameters.

## 5 Conclusions

**Summary.** This paper proposes a projection regularization loss to mitigate the risk of training collapse and trivial solutions in equivariant-based contrastive learning. We integrate equivariant representations into the invariant-based contrastive learning approach, proposing a novel equivariant-based contrastive learning method, CLeVER. CLeVER provides perturbation-related information without introducing inductive bias, significantly improving the training efficiency, generalization, and robustness of mainstream backbone models across various types and scales.

**Limitations and Future Works.** Despite the promising performance of CLeVER, the extraction of equivariant factors based on orthogonal loss remains obscure. Currently, we cannot explicitly map equivariant factors to specific augmentation operations. This may be due to the insufficient semantics in equivariant factors, leading to challenges in understanding and interpretation. Consequently, we plan to further investigate methods to extract equivariant factors in a more interpretable manner.

## References

- [1] G. Bai, W. Xi, X. Hong, X. Liu, Y. Yue, and S. Zhao. Robust and rotation-equivariant contrastive learning. *IEEE Transactions on Neural Networks and Learning Systems*, 2023.
- [2] S. Batzner, T. Smidt, L. Sun, J. Mailoa, M. Kornbluth, N. Molinari, and B. Kozinsky. Se(3)-equivariant graph neural networks for data-efficient and accurate interatomic potentials. Mar 2021. URL <http://dx.doi.org/10.21203/rs.3.rs-244137/v1>.
- [3] L. Bossard, M. Guillaumin, and L. Van Gool. Food-101 – mining discriminative components with random forests. In *European Conference on Computer Vision*, 2014.
- [4] M. Caron, H. Touvron, I. Misra, H. Jegou, J. Mairal, P. Bojanowski, and A. Joulin. Emerging properties in self-supervised vision transformers. In *2021 IEEE/CVF International Conference on Computer Vision (ICCV)*, Oct 2021. doi: 10.1109/iccv48922.2021.00951. URL <http://dx.doi.org/10.1109/iccv48922.2021.00951>.
- [5] T. Chen, S. Kornblith, M. Norouzi, and G. Hinton. A simple framework for contrastive learning of visual representations. In *International conference on machine learning*, pages 1597–1607. PMLR, 2020.
- [6] X. Chen and K. He. Exploring simple siamese representation learning. In *2021 IEEE/CVF Conference on Computer Vision and Pattern Recognition (CVPR)*, Jun 2021. doi: 10.1109/cvpr46437.2021.01549. URL <http://dx.doi.org/10.1109/cvpr46437.2021.01549>.
- [7] X. Chen, H. Fan, R. Girshick, and K. He. Improved baselines with momentum contrastive learning. *arXiv preprint arXiv:2003.04297*, 2020.
- [8] C.-Y. Chuang, J. Robinson, Y.-C. Lin, A. Torralba, and S. Jegelka. Debaised contrastive learning. *Advances in neural information processing systems*, 33:8765–8775, 2020.
- [9] R. Dangovski, L. Jing, C. Loh, S. Han, A. Srivastava, B. Cheung, P. Agrawal, and M. Soljačić. Equivariant contrastive learning. *arXiv preprint arXiv:2111.00899*, 2021.
- [10] A. Devillers and M. Lefort. Equimod: An equivariance module to improve self-supervised learning. Nov 2022.
- [11] J. Devlin, M.-W. Chang, K. Lee, and K. Toutanova. Bert: Pre-training of deep bidirectional transformers for language understanding. *arXiv preprint arXiv:1810.04805*, 2018.
- [12] A. Dosovitskiy, L. Beyer, A. Kolesnikov, D. Weissenborn, X. Zhai, T. Unterthiner, M. Dehghani, M. Minderer, G. Heigold, S. Gelly, J. Uszkoreit, and N. Houlsby. An image is worth 16x16 words: Transformers for image recognition at scale. *arXiv: Computer Vision and Pattern Recognition, arXiv: Computer Vision and Pattern Recognition*, Oct 2020.
- [13] J. E. Gerken, J. Aronsson, O. Carlsson, H. Linander, F. Ohlsson, C. Petersson, and D. Persson. Geometric deep learning and equivariant neural networks. *Artificial Intelligence Review*, page 14605–14662, Dec 2023. doi: 10.1007/s10462-023-10502-7. URL <http://dx.doi.org/10.1007/s10462-023-10502-7>.
- [14] P. Goyal, P. Dollár, R. Girshick, P. Noordhuis, L. Wesolowski, A. Kyrola, A. Tulloch, Y. Jia, and K. He. Accurate, large minibatch sgd: Training imagenet in 1 hour. *arXiv preprint arXiv:1706.02677*, 2017.

- [15] J.-B. Grill, F. Strub, F. Alché, C. Tallec, P. Richemond, E. Buchatskaya, C. Doersch, B. Avila Pires, Z. Guo, M. Gheshlaghi Azar, et al. Bootstrap your own latent—a new approach to self-supervised learning. *Advances in neural information processing systems*, 33:21271–21284, 2020.
- [16] J. Gui, T. Chen, J. Zhang, Q. Cao, Z. Sun, H. Luo, and D. Tao. A survey on self-supervised learning: Algorithms, applications, and future trends. *arXiv preprint arXiv:2301.05712*, 2023.
- [17] K. He, X. Zhang, S. Ren, and J. Sun. Deep residual learning for image recognition. In *Proceedings of the IEEE conference on computer vision and pattern recognition*, pages 770–778, 2016.
- [18] K. He, H. Fan, Y. Wu, S. Xie, and R. Girshick. Momentum contrast for unsupervised visual representation learning. In *Proceedings of the IEEE/CVF conference on computer vision and pattern recognition*, pages 9729–9738, 2020.
- [19] Y. Liu, Y. Tian, Y. Zhao, H. Yu, L. Xie, Y. Wang, Q. Ye, and Y. Liu. Vmamba: Visual state space model. *arXiv preprint arXiv:2401.10166*, 2024.
- [20] M.-E. Nilsback and A. Zisserman. Automated flower classification over a large number of classes. In *Proceedings of the Indian Conference on Computer Vision, Graphics and Image Processing*, Dec 2008.
- [21] M. Oquab, T. Darcet, T. Moutakanni, H. V. Vo, M. Szafraniec, V. Khalidov, P. Fernandez, D. HAZIZA, F. Massa, A. El-Nouby, M. Assran, N. Ballas, W. Galuba, R. Howes, P.-Y. Huang, S.-W. Li, I. Misra, M. Rabbat, V. Sharma, G. Synnaeve, H. Xu, H. Jegou, J. Mairal, P. Labatut, A. Joulin, and P. Bojanowski. DINOv2: Learning robust visual features without supervision. *Transactions on Machine Learning Research*, 2024. ISSN 2835-8856. URL <https://openreview.net/forum?id=a68SUt6zFt>.
- [22] O. M. Parkhi, A. Vedaldi, A. Zisserman, and C. V. Jawahar. Cats and dogs. In *IEEE Conference on Computer Vision and Pattern Recognition*, 2012.
- [23] O. Russakovsky, J. Deng, H. Su, J. Krause, S. Satheesh, S. Ma, Z. Huang, A. Karpathy, A. Khosla, M. Bernstein, A. C. Berg, and L. Fei-Fei. ImageNet Large Scale Visual Recognition Challenge. *International Journal of Computer Vision (IJCV)*, 115(3):211–252, 2015. doi: 10.1007/s11263-015-0816-y.
- [24] S. Sabour, N. Frosst, and G. Hinton. Dynamic routing between capsules. *Neural Information Processing Systems, Neural Information Processing Systems*, Oct 2017.
- [25] J. Shi, Q. Yan, L. Xu, and J. Jia. Hierarchical image saliency detection on extended cssd. *IEEE transactions on pattern analysis and machine intelligence*, 38(4):717–729, 2015.
- [26] C. Wah, S. Branson, P. Welinder, P. Perona, and S. Belongie. Technical Report CNS-TR-2011-001, California Institute of Technology, 2011.
- [27] J. Wang, S. Song, J. Su, and S. K. Zhou. Distortion-disentangled contrastive learning. In *Proceedings of the IEEE/CVF Winter Conference on Applications of Computer Vision*, pages 75–85, 2024.
- [28] L. Wang, H. Lu, Y. Wang, M. Feng, D. Wang, B. Yin, and X. Ruan. Learning to detect salient objects with image-level supervision. In *2017 IEEE Conference on Computer Vision and Pattern Recognition (CVPR)*, Jul 2017. doi: 10.1109/cvpr.2017.404. URL <http://dx.doi.org/10.1109/cvpr.2017.404>.
- [29] Y. Wang, X. Shen, S. X. Hu, Y. Yuan, J. L. Crowley, and D. Vaufreydaz. Self-supervised transformers for unsupervised object discovery using normalized cut. In *Proceedings of the IEEE/CVF Conference on Computer Vision and Pattern Recognition*, pages 14543–14553, 2022.
- [30] M. Weiler, P. Forré, E. Verlinde, and M. Welling. *Equivariant and Coordinate Independent Convolutional Networks*. 2023. URL [https://maurice-weiler.gitlab.io/cnn\\_book/EquivariantAndCoordinateIndependentCNNs.pdf](https://maurice-weiler.gitlab.io/cnn_book/EquivariantAndCoordinateIndependentCNNs.pdf).
- [31] T. Xiao, X. Wang, A. Efros, and T. Darrell. What should not be contrastive in contrastive learning. *International Conference on Learning Representations, International Conference on Learning Representations*, May 2021.
- [32] R. Xu, K. Yang, K. Liu, and F. He.  $e(2)$ -equivariant vision transformer. Jun 2023.
- [33] C. Yang, L. Zhang, H. Lu, X. Ruan, and M.-H. Yang. Saliency detection via graph-based manifold ranking. In *2013 IEEE Conference on Computer Vision and Pattern Recognition*, Jun 2013. doi: 10.1109/cvpr.2013.407. URL <http://dx.doi.org/10.1109/cvpr.2013.407>.

## Appendix

### 5.1 Qualitative Performance of Downstream Segmentation Tasks

Table 5 quantitatively demonstrates that, compared to DINO, CLeVER significantly improves performance on downstream segmentation tasks, especially when pre-trained with more complex augmentations. Figure 4 qualitatively illustrates that the attention-based saliency segmentation results of our proposed CLeVER are significantly better than those of DINO.

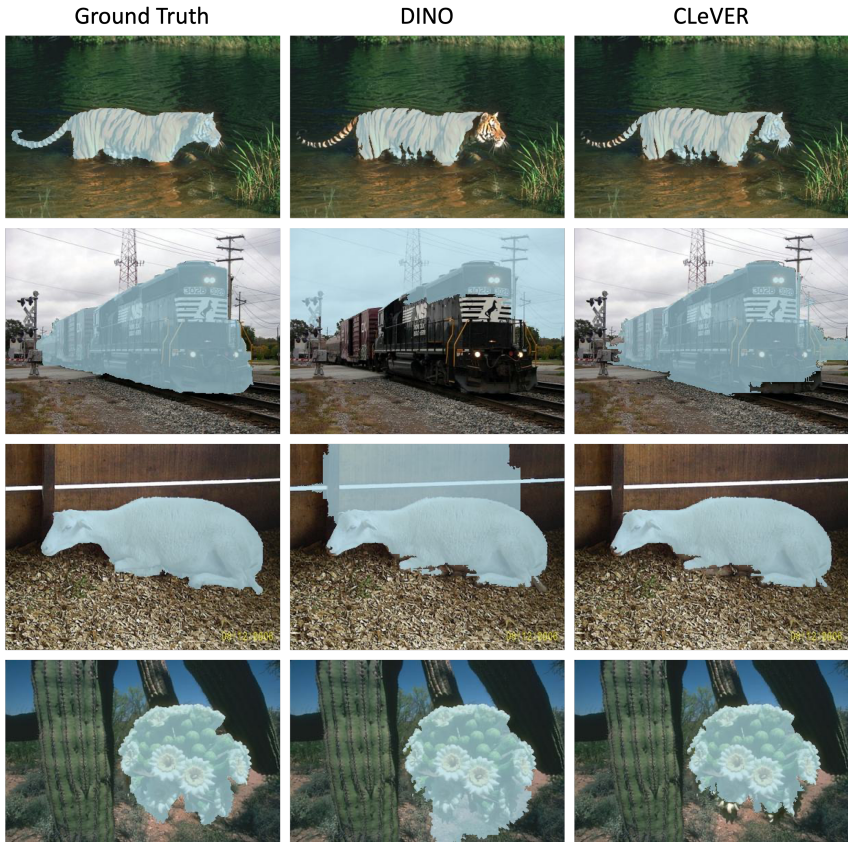


Figure 4: Qualitative performance of unsupervised saliency segmentation task.

### 5.2 Detailed Experimental Setups

Referring to DINO [4], when pretraining the model, we use SGD with base lr = 0.001, initial weight decay = 0.04, momentum = 0.9, and a cosine decay schedule on both IN-1k and IN-100 datasets. We conduct all experiments with a batch size of 128 per GPU on four NVIDIA A100 (80G) GPUs (or a batch size of 256 per GPU on 2 A100 GPUs), following the linear scaling rule [14]. For linear evaluation, we use a SGD optimizer with 100 epochs, lr = 0.002, weight decay = 0, momentum = 0.9, and batch size per GPU = 128. On the linear evaluation experiments, only the linear layer is trained. In addition, identical to DINO, we use a warm-up strategy for a more stable training process with 10 warm-up epochs. For fine-tune-based downstream experiments (semi-supervised learning with 1% and 10% labels and downstream classification tasks on CUB200 [26], Flowers102 [20], Food101 [3] and OxfordPet [22]), we use a SGD optimizer with 200 epochs, lr of backbone and linear layer = 0.001, weight decay = 0.0001, momentum = 0.9, with a batch size of 256 per GPU. If the experiments are conducted with a batch size of 128 per GPU on four NVIDIA GPUs, the memory is less than 40G per GPU and the training time is around 3.5 hours per 100 epochs for ViT-small on IN100 datasets (The training time is also related to the type of hard drive.)

### 5.3 Augmentation Settings

Compared to default augmentation setting used in DINO (*i.e.*, BAug), the CAug has an additional “transforms.RandomRotation(degrees=(-90, 90))” for all input images, and the CAug+ has additional “transforms.RandomRotation(degrees=(-90, 90))” and “transforms.RandomApply([transforms.ElasticTransform(alpha=100.0)], p=0.5)” for all input images.